iScience

CellPress
OPEN ACCESS

Article

Gene signature reveals decreased SOX10-dependent transcripts in malignant cells from immune checkpoint inhibitor-resistant cutaneous melanomas

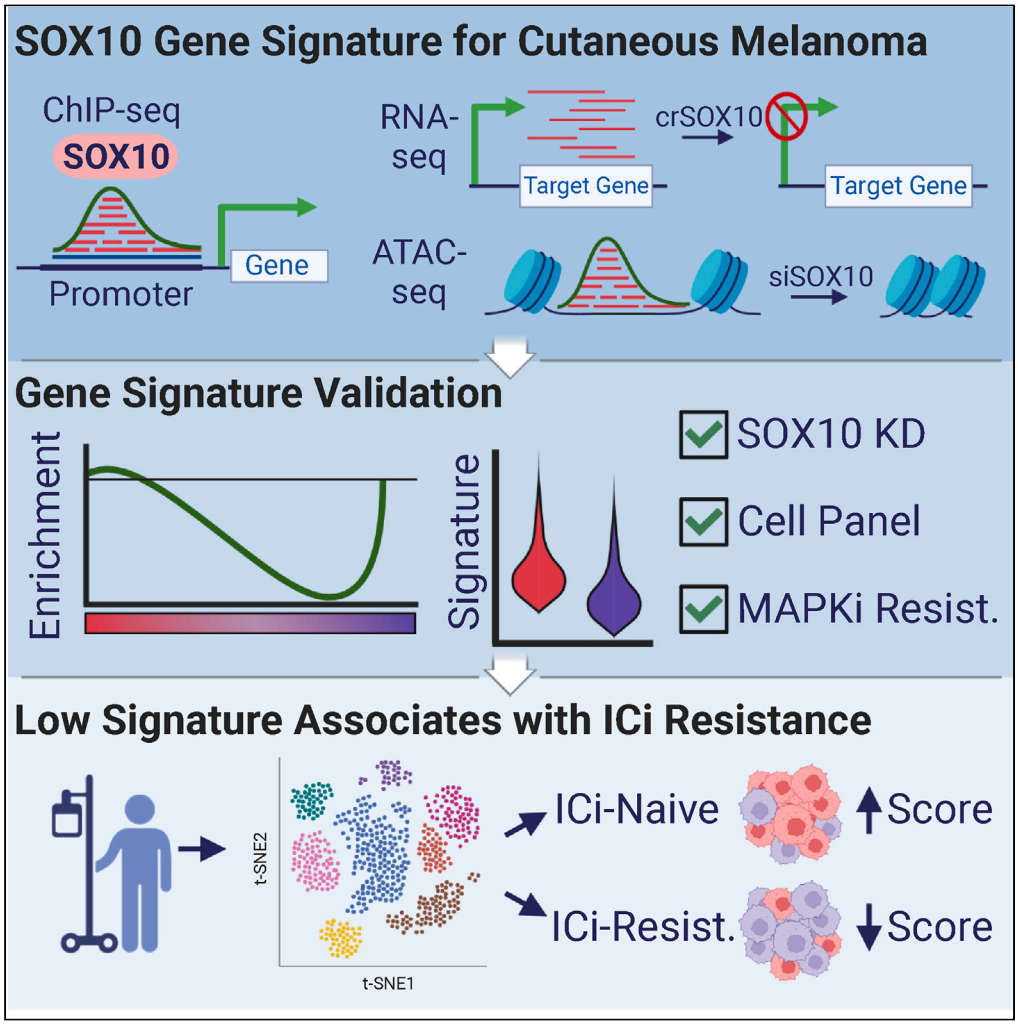

Timothy J. Purwin, Signe Caksa, Ahmet Sacan, Claudia Capparelli, Andrew E. Aplin

andrew.aplin@jefferson.edu

Highlights

Multi-omic analysis was used to generate a SOX10 gene signature in cutaneous melanoma

The SOX10 signature was validated for use with bulk and single-cell RNA-seq data

Lower SOX10 signature scores were observed in ICi-resistant melanoma patient tumors

SOX10 loss may promote cross-resistance between MAPKi and ICi therapies in melanoma

Purwin et al., iScience 26, 107472
September 15, 2023
https://doi.org/10.1016/j.isci.2023.107472

iScience

CellPress
OPEN ACCESS

Article

Gene signature reveals decreased SOX10-dependent transcripts in malignant cells from immune checkpoint inhibitor-resistant cutaneous melanomas

Timothy J. Purwin,[1,2] Signe Caksa,[1] Ahmet Sacan,[2] Claudia Capparelli,[3,4] and Andrew E. Aplin[1,4,5,*]

SUMMARY

Evidence is mounting for cross-resistance between immune checkpoint and targeted kinase inhibitor therapies in cutaneous melanoma patients. Since the loss of the transcription factor, SOX10, causes tolerance to MAPK pathway inhibitors, we used bioinformatic techniques to determine if reduced SOX10 expression/activity is associated with immune checkpoint inhibitor resistance. We integrated SOX10 ChIP-seq, knockout RNA-seq, and knockdown ATAC-seq data from melanoma cell models to develop a robust SOX10 gene signature. We used computational methods to validate this signature as a measure of SOX10-dependent activity in independent single-cell and bulk RNA-seq SOX10 knockdown, cell line panel, and MAPK inhibitor drug-resistant datasets. Evaluation of patient single-cell RNA-seq data revealed lower levels of SOX10-dependent transcripts in immune checkpoint inhibitor-resistant tumors. Our results suggest that SOX10-deficient melanoma cells are associated with cross-resistance between targeted and immune checkpoint inhibitors and highlight the need to identify therapeutic strategies that target this subpopulation.

INTRODUCTION

Cutaneous melanoma (CM) is the deadliest form of skin cancer. v-Raf murine sarcoma viral oncogene homolog B (BRAF) driver mutations occur in approximately 50% of CM patients[1] and constitutively activate the BRAF-mitogen-activated extracellular signal-regulated kinase (MEK)-extracellular signal-regulated kinase (ERK)/mitogen-activated protein kinase (MAPK) pathway. Targeted MAPK pathway inhibitors (BRAFi and MEKi) elicit an initial response, but tumors frequently re-emerge and disease progression occurs.[2] In minimal residual disease established during targeted therapy treatment, cell plasticity and transcriptomic reprogramming enable drug tolerance and eventual tumor re-growth.[3] Loss of sex-determining region Y protein (SRY)-box transcription factor 10 (SOX10) expression mediates drug tolerance to MAPK pathway inhibitors in melanoma and is evident in acquired resistance.[3–5] SOX10 is a transcription factor (TF) that is important for lineage differentiation of neural crest cells into melanocytes.[6–8]

Gene signatures are often generated from curated, experimental, or sequencing results, such as signaling pathways or phenotypic cell states.[3,9–12] Some signatures have been generated from differentially expressed genes between conditions or sample groups.[13,14] However, more detailed evaluations are necessary when developing TF gene signatures for use with expression data since not all differentially expressed genes are direct targets of a TF and not all predicted TF targets have altered gene expression.[15] Integration of chromatin immunoprecipitation sequencing (ChIP-seq) TF binding peaks and RNA sequencing (RNA-seq) data has improved the understanding of gene regulatory networks.[16–18] Additionally, disease-specific models need to be considered when developing a TF gene signature due to the differences in TF binding sites that are observed between cell lines from varying tissues.[19] Using data derived from multiple models of the same disease is important for overcoming limitations from noise and variability in the data and revealing common events[20] and generates robust gene signatures.

Immune checkpoint inhibitors (ICi) are effective in up to 60% of CM patients.[21] Copy number loss and loss-of-function mutations in antigen presentation and interferon receptor signaling genes have been observed in some ICi-resistant patient samples.[22,23] Single-cell RNA sequencing (scRNA-seq) studies investigating mechanisms of ICi resistance have characterized changes in the immune compartment, including T cell

[1]Department of Pharmacology, Physiology, and Cancer Biology, Thomas Jefferson University, Philadelphia, PA 19107, USA

[2]School of Biomedical Engineering, Science and Health Systems, Drexel University, Philadelphia, PA 19104, USA

[3]Medical Oncology, Thomas Jefferson University, Philadelphia, PA 19107, USA

[4]Sidney Kimmel Cancer Center, Thomas Jefferson University, Philadelphia, PA 19107, USA

[5]Lead contact

*Correspondence: andrew.aplin@jefferson.edu

https://doi.org/10.1016/j.isci.2023.107472

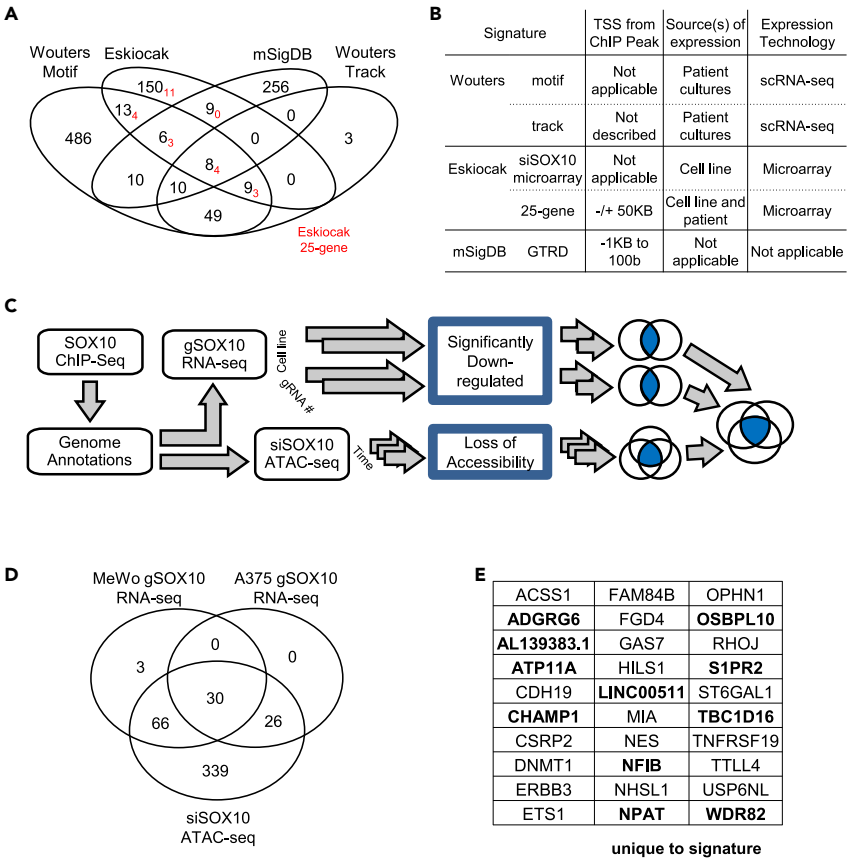

Figure 1. Developing a robust SOX10 gene signature

(A) A Venn diagram showing minimal overlap in the number of genes from publicly available SOX10 gene signatures.

(B) A table showing the core differences between methods used for developing the gene signatures in (A).

(C) A workflow diagram displaying the methods for developing the robust SOX10 regulatory gene signature.

(D) Venn diagram plot showing the genes overlapping between the gSOX10 RNA-seq and ATAC-seq results.

(E) The list of the 30 genes identified using the workflow in (C). Genes not present in (A) are shown in bold.

exhaustion or dysfunction and the presence of a dendritic cell population.[24–26] Cross-resistance between targeted and ICi therapies has been identified,[27] but the malignant cell populations contributing to this cross-resistance remain poorly characterized. Elevated levels of epithelial-to-mesenchymal transition (EMT) genes have been associated with immunotherapy resistance[28] as well as with the loss of SOX10 expression.[29] Our previous findings showed that SOX10 loss mediates drug tolerance to MAPK inhibitors. Here, we examined whether loss of SOX10 expression is associated with ICi resistance. We developed a robust SOX10 gene signature by integrating multiple datasets and validated the signature in independent datasets and cell-based models. Evaluation of patient scRNA-seq data revealed that ICi-resistant patient tumors have lower SOX10-dependent transcripts than treatment-naive tumors. SOX10 immunohistochemistry (IHC) staining confirmed a higher prevalence of SOX10-deficient melanoma cells in tumor samples following ICi therapy.

RESULTS

Generation of a SOX10 gene signature

Literature and database searches revealed multiple SOX10 gene signatures; however, a comparison of these signatures showed minimal overlap of genes (Figure 1A). Eskiocak et al.[30] developed a down-regulated 25 gene signature that was defined by overlapping a small interfering RNA (siRNA) knockdown of SOX10 (siSOX10) gene expression microarray signature with SOX10 ChIP-seq and SOX10 correlation results from patient gene expression datasets. Wouters et al.[31] developed two SOX10 signatures referred to as motif and track. Both were created using scRNA-seq data and SCENIC,[32] a computational method

that identifies potential TF targets based on co-expression, with an option to provide TF and putative gene target information. The motif- and track-based signatures incorporate TF regulatory networks identified by motif enrichment and ChIP-seq peak calling, respectively. The molecular signature database (mSigDB)[33] curated a list of genes that contain a SOX10 ChIP-seq peak between 1,000 bases upstream and 100 bases downstream of the transcription start site (TSS). Core differences in the methods used to develop these signatures include the distances from a TSS to a SOX10 ChIP-seq peak as well as the sources and technologies used to produce gene expression data (Figure 1B). Due to the differences in these signatures, we decided to generate a SOX10 signature that incorporates multiple types of datasets.

We integrated a comprehensive list of curated annotation and biomolecular datasets including gene, transcript, and regulatory information along with ChIP-seq, assay for transposase-accessible chromatin sequencing (ATAC-seq), and RNA-seq data (Figure 1C, see STAR Methods). Time series SOX10-knockdown ATAC-seq data showed a consistent decrease in open chromatin at SOX10 ChIP-seq target genes (Figure S1A). In Capparelli et al.,[29] four SOX10-null melanoma models were generated using two different SOX10 CRISPR guide RNAs (gSOX10) in MeWo and A375 cell lines. From the corresponding RNA-seq data, we performed differential gene expression analysis between the gSOX10 and parental cell line samples and considered significantly down-regulated SOX10 ChIP-seq target genes common to all four models as SOX10 targets (Figure S1B, Table S1). Upon integrating these results, we developed a refined SOX10-null signature consisting of 30 genes (Figures 1D and 1E, Table S1). While a majority of the genes in the signature were present in at least one other SOX10 gene signature, 11 genes were unique (Figure S1C). Analysis of our signature genes via database for annotation, visualization and integrated discovery (DAVID)[34] revealed enrichment for actin cytoskeleton organization (p value = 1.6E-3) and Schwann cell differentiation (p value = 9E-3) gene sets (Figure S1D). Although down-regulation or lack of expression was observed for some antigen-related genes in gSOX10 samples, the genes were not predicted targets based on SOX10 ChIP-seq data (Figure S1E).

Robustness of the signature in SOX10-knockdown datasets

To determine the robustness of our signature, we first evaluated it using independent SOX10-perturbed CM datasets. We used the gene set enrichment analysis (GSEA) method,[33,35] which takes a list of signature genes and utilizes a rank-based statistical method to calculate an overall score. We tested a dataset from Wouters et al.[31] consisting of RNA-seq data for six CM cell lines, each transfected with either SOX10 targeting or control siRNA for 72 h. Some of the SOX10-knockdown samples had residual SOX10 transcript levels comparable to control levels in other cell lines (Figure S2A). Due to this and to control for variability in the cell lines, we used a paired-sample model when performing differential expression analysis to generate a ranked list. GSEA results showed significant negative enrichment (p value <0.001) of the SOX10 signature following SOX10 knockdown (Figure 2A). We then investigated an RNA-seq dataset from Sun et al.[5] that contains two SOX10-knockdown samples and a parental control sample. After processing the data from the raw reads, we performed GSEA using the log2-transformed ratio as the weight metric for the pre-ranked list of genes. Despite a marginal difference in SOX10 expression between the SOX10-knockdown and parental samples (Figure S2B), we observed that the SOX10 signature was close to significant negative enrichment (p value = 0.099, Figure 2B). Similar results were observed for the other SOX10 gene signatures (Figures S2C and S2D). After discovering that there was negative enrichment of our signature following SOX10 knockdown in two independent datasets, we concluded that our signature robustly captures gene expression changes following SOX10 perturbation in CM.

To test our signature's ability to capture SOX10 activity levels in scRNA-seq data, we used AUCell,[32] which calculates the area under the ROC curve for genes in a signature using a pre-defined top percentage of genes sorted by expression level to generate a signature score. In doing this, we could compensate for the known dropout of transcripts in scRNA-seq data.[36] Four SOX10-knockdown scRNA-seq datasets from Wouters et al.[31] were evaluated for differences in signature scores following siSOX10. We observed significant changes in SOX10-dependent transcripts for nearly all pairwise comparisons against control samples (Figures 2C-F). These results confirm the ability of our signature to capture SOX10 levels and/or activity in scRNA-seq data.

Robustness of the signature in cell line panel datasets

We next evaluated our signature in multiple large-scale melanoma cell line cohorts to determine its ability to distinguish endogenous differences in SOX10-dependent transcripts versus those induced

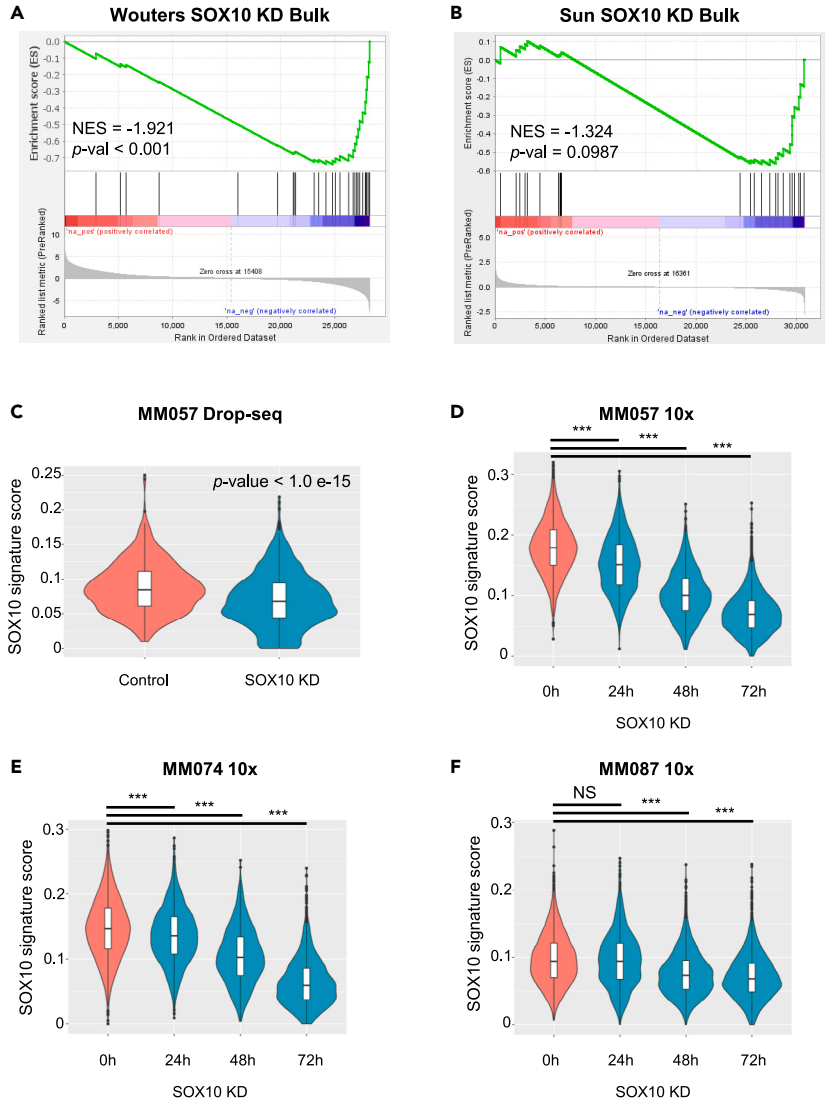

Figure 2. SOX10 signature is enriched in independent SOX10-knockdown datasets

(A) An enrichment plot showing down-regulation of our signature in SOX10 knockdown paired-sample results from Wouters et al.[31] dataset. The plot shows a running enrichment score along a ranked gene list with weights according to a scoring metric. Tic marks represent genes while red and blue represent up- and down-regulated genes, respectively, following SOX10 knockdown.

(B) An enrichment plot showing down-regulation of the signature in SOX10 knockdown fold change results from Sun et al.[5] dataset.

(C) Violin plot displaying lower SOX10 activity scores following knockdown in Drop-seq scRNA-seq data for MM057 cell line samples.

(D-F) Violin plots displaying lower SOX10 activity scores in knockdown time course 10x Genomics scRNA-seq data for MM057 (D), MM074 (E), and MM087 (F) cell line samples. Significance was assessed by the Mann-Whitney test, *p < *0.05*, **p < *0.01*, ***p < *0.001*. NS: Not Significant. Violin plots contain box and whiskers (interquartile range, median and minimum/maximum values).

experimentally. This evaluation would allow us to determine whether our signature was able to: i) identify melanoma cell lines with inherently low SOX10 and ii) detect SOX10 loss in a diverse pool of cell lines more representative of patient populations. We explored two independent bulk RNA-seq datasets with over 50 CM cell line samples. The first dataset includes CM cell line samples from the Cancer Dependency Map (DepMap).[20] Six out of the 62 CM samples had little to no SOX10 expression (Figure 3A). We conducted hierarchical clustering of normalized expression data for our signature genes, which resulted in the top

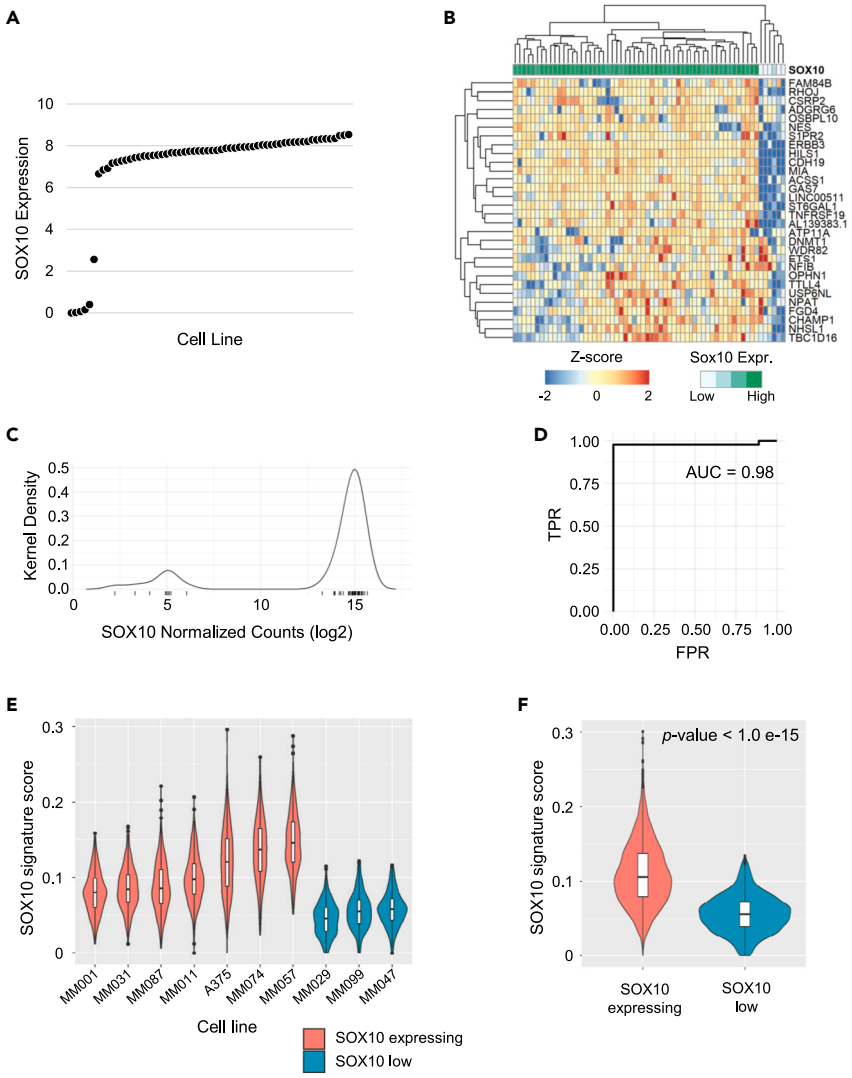

Figure 3. SOX10 signature stratifies samples by SOX10 expression in multiple cell line cohorts

(A) A scatterplot showing normalized SOX10 expression in CM samples from DepMap,[20] with cell line samples ordered by SOX10 expression.

(B) A heatmap showing cell lines from (A) separating by SOX10 expression following hierarchical clustering.

(C) A frequency plot showing the kernel density of the number of samples in a bimodal distribution based on SOX10 expression from the Tsoi et al.[37] dataset. Tick marks on the x axis indicate a cell line sample.

(D) An ROC curve showing the SOX10 gene signature score accurately identifying cell lines in (C) from high and low SOX10 expression groups.

(E) Violin plot displaying SOX10 activity scores for each cell line individually from Wouters et al.[31] dataset.

(F) Violin plot showing significantly lower levels of SOX10 activity scores in SOX10-low vs. SOX10-expressing cell lines from E. Significance was assessed by the Mann-Whitney test, *p < *0.05*, **p < *0.01*, ***p < *0.001*. NS: Not Significant. Violin plots contain box and whiskers (interquartile range, median and minimum/maximum values).

branchpoint separating the cell lines into clusters according to SOX10 expression (Figure 3B). For the second dataset, which was initially presented in Tsoi et al.,[37] we confirmed multimodality in the expression of SOX10 and subsequently stratified cell lines into low (n = 9) and high (n = 44) groups using the anti-mode from a bimodal kernel density as a cutoff (Figure 3C). After calculating gene signature scores for each cell line using the single-sample GSEA (ssGSEA)[38] method, we observed that our signature was highly accurate (area under the curve [AUC] 0.98) at identifying samples originating from SOX10-low and SOX10-high groups (Figure 3D). These results show that our signature can differentiate cell lines with low versus high endogenous SOX10 expression in bulk RNA-seq datasets, suggesting strong reproducibility.

To determine whether our signature differentiates SOX10 activity in additional settings, we evaluated scRNA-seq data from patient-derived cell lines known to have varying SOX10 expression levels (Figure S3A).[31] After calculating SOX10 activity scores using AUCell, pairwise comparisons showed significant differences between each of the SOX10-low (n = 3) and SOX10-expressing (n = 7) cell lines (Figures 3E and S3B). There was also a significant decrease (p value <1.0 e−15) in SOX10 activity when comparing all cells from SOX10-low and SOX10-expressing lines (Figure 3F). This confirms the ability of our signature to capture SOX10 activity in a scRNA-seq dataset with cell lines lacking endogenous SOX10.

We tested how our signature performed against SOX10 mRNA expression as a predictor of SOX10-dependent transcription activity. To this end, we used SOX10 levels from proteomics data in SOX10-expressing CM cell lines from the DepMap database.[20,39] We performed correlation analysis of SOX10 protein expression data with SOX10 RNA-seq levels and signature scores calculated using ssGSEA from RNA-seq data. Although not significant, we observed a higher correlation with SOX10 protein expression levels using the signature scores than with SOX10 RNA expression data (Figure S3C), indicating that, when considering RNA-seq data, our signature may be a better readout of SOX10-dependent transcription than SOX10 expression alone.

Evaluation of the signature in SOX10-null targeted inhibitor-resistant datasets

Since the loss of SOX10 has been associated with MAPK inhibitor resistance in melanoma,[6–8] we evaluated how well our signature captures SOX10 loss in drug resistance models. We tested multiple drug-resistant CM cell lines, established from two separate *in vivo* experiments that lack SOX10 expression (Figures S4A and S4B).[29] These include tumors that are resistant to the BRAFi, PLX8394,[40] or the BRAFi + MEKi combination treatment, PLX4720 + PD0325901.[41] As before, GSEA was used with pre-ranked lists to determine the enrichment of our signature in each resistant cell line. We observed significant negative enrichment (p value <0.001) in both cell lines that were resistant to PLX8394 (Figure 4A) as well as the two cell lines resistant to PLX4720 + PD0325901 (Figure 4B). These results show that our signature is robust at capturing loss of SOX10-dependent transcriptional events in drug-resistant bulk RNA-seq data.

In line with our evaluation of SOX10-knockdown and cell line panel data, we sought to determine whether our signature would reveal lower SOX10-dependent transcription in drug-resistant cell line models using scRNA-seq data from Schmidt and Mortensen et al.[42] Untreated and BRAFi −/+ MEKi-resistant A375 samples were processed from raw sequencing data, with resistant samples having fewer cells with SOX10 expression (Figures S4C and S4D). Analysis of SOX10 activity scores revealed a significant decrease (p value <1.0 e−15) in the resistant samples when considering each resistance model separately (Figure 4C) or as a single group (Figure 4D). These results show the ability of our signature to capture SOX10-dependent transcription in BRAFi −/+ MEKi-resistant melanoma samples in scRNA-seq data.

Lower SOX10 activity levels in ICi-resistant patient tumors

After confirming the ability of our signature and AUCell to capture SOX10-dependent differences in scRNA-seq datasets, we sought to determine if there was an association between malignant cells from ICi-treated patient tumor samples and decreased SOX10 levels/activity. To this end, we analyzed scRNA-seq cohorts from Alvarez-Breckenridge et al.[43] and Jerby-Arnon et al.[44] We followed this up by evaluating IHC data containing SOX10 staining of patient tumor malignant cells from Capparelli et al.[29]

We explored the Alvarez-Breckenridge et al. dataset for an association between therapeutic response and SOX10 activity scores. This dataset contains resected melanoma brain metastasis samples that were previously classified as treated with ICi (Post-ICi) or ICi naive.[43] Standard clinical care prompted tumor resection in each case, and all Post-ICi tumors were described as requiring resection due to intracranial progression.[43] Clinical responses were previously identified for each patient as Responder, Partial-responder, and Non-responder, and none of the patients had both ICi-naive and Post-ICi samples.[43] Of the three ICi-naive patients that later received ICi (Pre-ICi), one was a Responder and the others were Non-responders.[43] Two of the ICi-naive patients received radiotherapy prior to resection. Following criteria used in Jerby-Arnon et al.,[44] we limited the tumor samples to those with at least 50 malignant cells for further analyses. SOX10 signature scores in malignant cells were heterogeneous across treatment groups (Figure S5A). When combining samples by groups defined in Alvarez-Breckenridge et al.,[43] the lowest average signature score was in the Pre-ICi responder (Figure 5A), which was significantly lower than that in the Pre-ICi Non-responder group (p value = 2.26 e−3). Although not statistically significant (p value = 0.066), there was a

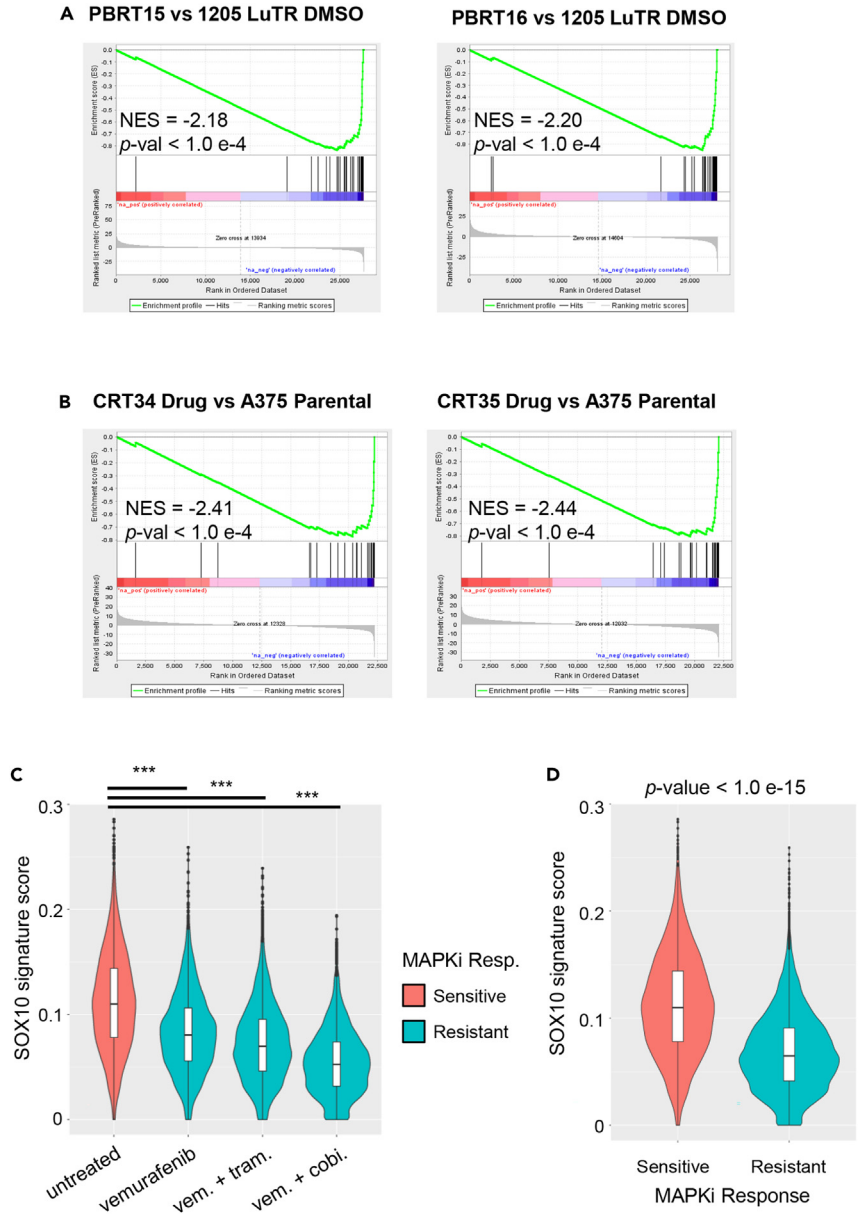

Figure 4. SOX10 signature reproducible in SOX10-null drug-resistant datasets

(A) Gene set enrichment plots showing the comparisons of BRAFi-resistant samples vs. parental 1205 Lu TR for PBRT#15 (left panel) and PBRT#16 (right panel) cell lines from Hartsough et al.[40]

(B) Gene set enrichment plots showing the comparisons of BRAFi + MEKi-resistant samples vs. parental A375 for CRT#34 (left panel) and CRT#35 (right panel) cell lines from Sanchez et al.[41]

(C and D) Violin plots showing significantly lower levels of SOX10 activity scores in pairwise (C) and overall (D) comparisons between BRAFi −/+ MEKi-resistant and untreated control cells from Schmidt and Mortensen et al.[42] dataset. Significance was assessed by the Mann-Whitney test, *p < *0.05*, **p < *0.01*, ***p < *0.001*. NS: Not Significant. Violin plots contain box and whiskers (interquartile range, median and minimum/maximum values).

slightly lower signature score in the Post-ICi Non-responders when compared to Post-ICi Partial-responders (Figure 5A). These results suggested a trend for lower SOX10 levels/activity in the Non-responders versus Partial-responders post-ICi treatment.

We further investigated the Alvarez-Breckenridge et al. dataset to determine if there was an association between SOX10 signature scores and on ICi. We grouped ICi-naive samples together and Post-ICi samples

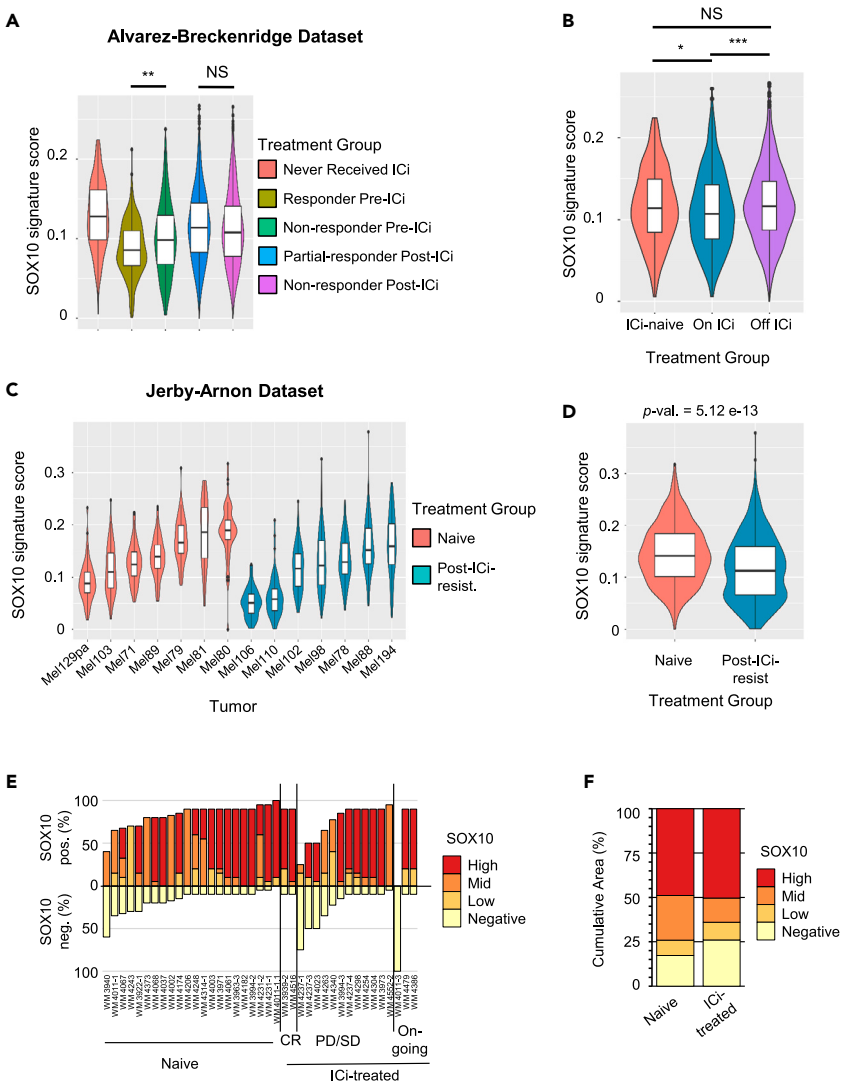

Figure 5. SOX10 signature reveals resistance to ICi therapy

(A) Violin plots of SOX10 signature score values for malignant cells from resected brain metastases scRNA-seq data with samples stratified into groups defined in Alvarez-Breckenridge et al.[43]

(B) Violin plots showing lower SOX10 signature score values in malignant cells from On ICi tumors when compared to ICi-naive and Off ICi tumors.

(C) Violin plots of SOX10 signature score values for tumors ordered by median score and grouped by treatment type from Jerby-Arnon et al.[44] dataset.

(D) Violin plots showing lower SOX10 signature score values in cells from ICi-resistant compared to treatment-naive patient tumors.

(E) Waterfall plot depicting the percent of malignant cells staining positive (low, mid, and high) or negative for SOX10 in treatment-naive and ICi-treated samples.

(F) Bar plot displaying a higher percentage of SOX10 negative malignant cells in ICi-treated tumors compared to treatment-naive. Significance was assessed by the Mann-Whitney test, *p < *0.05*, **p < *0.01*, ***p < *0.001*. NS: Not Significant. Violin plots contain box and whiskers (interquartile range, median and minimum/maximum values).

based on the patients' systemic therapy at the time of resection,[43] resulting in ICi-naive (n = 8), On MAPKi (n = 2), On ICi (n = 6), and Off ICi (n = 12) tumor samples (Figure S5A). We excluded the on MAPKi samples from the Off ICi group since there is the potential for lower SOX10 signature scores in tumors progressing while on MAPKi therapy. The SOX10 signature score was significantly lower in the On ICi group when compared to the ICi-naive (p value = 0.0172) and Off ICi (p value = 2.16 e−4) groups (Figure 5B). Similar

results were observed when analyzing SOX10 expression between groups (Figure S5B). This suggests that there may be lower SOX10 in tumors on ICi.

To determine if there was an association between SOX10 levels/activity and ICi resistance, we evaluated the Jerby-Arnon et al.[44] dataset, which contains patient tumor samples classified as treatment-naive or ICi-resistant.[44] SOX10 signature scores in malignant cells were heterogeneous across treatment groups (Figure 5C); however, there was a significantly lower (p-val = 5.12 e−13) SOX10 signature score in the malignant cells from ICi-resistant samples (Figure 5D). Similar results were observed when using SOX10 gene expression data to compare ICi-resistant to ICi-naive samples (Figure S5C). This suggests that there is lower SOX10 in ICi-resist samples.

To extend our findings of lower SOX10-dependent transcript levels in ICi-treated patient tumors, we evaluated SOX10 expression in IHC data. A total of 22 samples were from patients without any past treatment (treatment-naive). Of 20 samples from patients who previously received ICi therapy, three were excluded due to patients either stopping ICi therapy because of adverse events (n = 1) or not having clinical response and treatment status information (n = 2). For the remaining samples from patients who previously received ICi therapy (ICi-treated), those from patients on ICi but without clinical response information were included and grouped as ''ongoing'' (n = 3). Using the latest ICi clinical response information available, samples were grouped into complete responders (CRs) (n = 2) and progressive or stable disease (PD/SD) (n = 12). Two of the PD samples were collected after 1–2 cycles of ICi therapy, while one patient with SD remained on treatment. Similar to both scRNA-seq datasets, we observed heterogeneous SOX10 staining across treatment groups (Figure 5E). Overall, we observed a higher percentage of SOX10-negative cells in ICi-treated (26%) compared to treatment-naive (17.3%) tumors (Figure 5F). We also detected a higher percentage of SOX10-negative cells in the PD/SD samples (25.2%) when compared to CR (10%) as well as the treatment-naive samples (Figure S5D). Therefore, we conclude that there are more malignant cells with no SOX10 expression in ICi-treated patient tumors and more malignant cells with no SOX10 in PD/SD compared to CR in ICi-treated samples.

We also examined the IHC data to determine if there was an association between SOX10 and On ICi tumors. Some patients had samples from different time points (Figures S5E–S5G). In one of two patients that had matched treatment-naive and ICi-treated tumor samples, all of the malignant cells from the On ICi tumor were SOX10 negative (Figure S5E). The second of these patients had a slight increase in the percent of SOX10-negative cells in the ICi-treated, Off ICi sample (Figure S5F). One patient with progressive disease had samples collected during and after ICi therapy (Figure S5G) with the On ICi sample having the highest percentage of SOX10 negative malignant cells. This suggests that there may be more malignant cells lacking SOX10 while on ICi treatment.

DISCUSSION

Cross-resistance between targeted kinase inhibitors and immunotherapy has been recognized,[27] but there is a gap in knowledge about mechanisms mediating cross-resistance effects. We have previously shown that SOX10 loss mediates tolerance to targeted therapy and is a common feature of acquired resistance to BRAFi + MEKi in melanoma. By integrating ChIP-seq, ATAC-seq, and RNA-seq data, we developed a robust SOX10 gene signature. We validated our signature as a measure of SOX10-dependent transcription activity in bulk and scRNA-seq datasets using SOX10-knockdown, cell line panel, and targeted therapy-resistant samples. We also detected decreased SOX10 signature scores in ICi-resistant patient tumors in two independent scRNA-seq datasets. Although not all ICi-resistant patient tumors showed lower levels of SOX10-dependent transcriptional activity, the trend for a lower SOX10 signature score and lower SOX10 IHC staining was consistent between these independent cohorts of ICi-resistant tumors.

All of the gene signatures correlated with SOX10 expression, but we note differences that may be attributed to the types of genomic measurements applied and the analysis methods used to process the data. Specifically, the use of transcriptomic data in a multi-omic signature may lead to the exclusion of several genes found in a ChIP-seq-based signature despite the distance threshold between ChIP-seq peaks and TSS locations in the multi-omic signature initially encapsulating the ChIP-seq signature. The computational methods used to identify TF peaks are also a factor; a motif-based approach produced more than a 5-fold increase in the number of genes compared to a ChIP-seq-based approach. We have overcome some difficulties in determining SOX10 transcriptional targets by using curated promoter

regions,[45] which increases the likelihood that SOX10 is regulating the gene. A limitation of our approach is that the curation process includes the number of ChIP-seq peaks identified at a genomic location when determining a promoter region, meaning that other TFs may potentially regulate the same gene. This limitation was overcome by additionally incorporating ATAC-seq data, which reveal whether any other TFs are bound to the promoter of a predicted SOX10 target gene and strengthened the ability to capture SOX10 activity levels.

The enrichment of actin cytoskeleton organization and Schwann cell differentiation genes in our signature correlates with processes that occur during phenotypic plasticity in melanoma[31] as well as SOX10's known importance in Schwann cells.[46,47] Erythroblastic leukemia viral oncogene homologue (ERBB3) was present in our signature set and is a well-documented transcriptional target of SOX10[48,49] that appeared in each of the SOX10 signatures. However, melanocyte inducing transcription factor (MITF), which was also present in all other signatures, was not significantly lower in the A375 gSOX10 comparisons and was consequently absent from our signature. Others have shown that A375 cell lines have low MITF mRNA levels at baseline.[31,50] Our results also identified genes not previously observed as predicted targets of SOX10 in melanoma, including Sphingosine-1-Phosphate Receptor 2 (S1PR2) and Adhesion G Protein-Coupled Receptor G6 (ADGRG6). Stimulation of S1PR2 inhibits Rac and activates RhoA in B16F10 mouse melanoma cells, reducing migration and invasion.[51] ADGRG6 binds to type-IV collagen,[52] and SOX10 and ADGRG6 have been associated with Schwann cell development and myelination.[46,47] The effect of decreased ADGRG6 and S1PR2 expression in SOX10-deficient melanoma cell migration awaits further testing.

The effect of SOX10 levels/transcriptional output on the immune microenvironment in CM is poorly understood. SOX10 expression promotes tumor growth in immune-competent mouse models of melanoma, suggesting immune evasion of SOX10-high tumors.[53,54] However, SOX10-dependent effects on programmed cell death ligand 1 (PD-L1) expression,[55] the complexity of tumor heterogeneity,[56] and T cell antigen recognition[57] may all contribute to observing decreased SOX10 activity in ICi-resistant patient tumors. SOX10-regulated genes identified in our signature, such as CDH19, could play a role in evading the immune system. In Frangieh et al.,[58] CRISPR screens revealed enrichment of CDH19 along with other genes with known loss-of-function tumor-infiltrating lymphocyte (TIL)-mediated ICi-resistance mechanisms. It remains to be determined if SOX10 loss is a driver of ICi resistance. SOX10-deficient melanoma cells may also evade the immune system in an antigen-specific manner. A reversible antigen down-modulation mechanism has been observed as a resistance mechanism to adoptive T cell transfer therapy in CM,[59] with characteristics similar to SOX10-deficient cells. These include the lack of the tumor-associated-antigens melanoma antigen recognized by T-cells (MART-1) and gp100 genes, melan-A (MLANA) and premelanosome protein (PMEL), which were down-regulated following SOX10 knockout in RNA-seq data. SOX10, as well as MLANA, were among several major histocompatibility complex (MHC) class-I antigen processing pathway genes consistently enriched in a CRISPR screen that revealed resistance or non-responsiveness to $CD8^+$ T cell-mediated killing.[60] The enrichment of SOX10 and MLANA loss is likely the result of evasion from an immunodominant-like T cell response. A similar immune escape mechanism was observed in a patient with an immunodominant tyrosinase-specific T cell response in a metastatic tumor that developed six years after a metastatic tumor with an MART-1-specific response.[61] These immunodominant properties will have implications on the field as recent clinical studies have revealed that neoadjuvant treatments prolong the tumor-free survival of CM patients.[62] Although SOX10 may contribute to resistance, other factors are also important for ICi response. For example, patient MEL027 exhibited a low overall SOX10 activity score yet responded to ICi therapy.[43] Thus, SOX10 signature scores may not be a predictor of intrinsic resistance to ICi therapy, although we note that patient MEL027 had multiple markers for a favorable response, including a high level of mutational burden, passing a minimum cutoff for the percentage of PD-L1-expressing malignant cells, and high levels of T cell infiltration. These results are from limited sample sizes, and future studies would benefit from analyzing data from patient-matched pre- and post-treatment samples.

Potential therapeutic options for targeting SOX10-deficient melanoma cells include placenta growth factor-2 ($PlGF\text{-}2_{123\text{-}144}$)-ICi conjugates and birinapant, an antagonist of the inhibitor of apoptosis protein (IAP) family of proteins. $PlGF\text{-}2_{123\text{-}144}$ conjugates display high binding affinities to not only collagens I-IV but also fibronectin,[63] an extracellular matrix protein produced by SOX10-negative CM cells.[29] Its use showed increased efficacy in the B16F10 murine CM model,[63] which is a mesenchymal-like cell line inherently less responsive to ICi therapies.[64] Birinapant has been shown to target SOX10-deficient cells and increase the durable efficacy of MAPK pathway targeted therapy *in vivo* and *in vitro*.[29] Birinapant acts on tumor cells independent of a cytotoxic immune response suggesting that its effectiveness may not rely on the presence of tumor-infiltrating lymphocytes.

In conclusion, we developed a core list of genes regulated by SOX10 in CM. Some genes identified were not previously associated with SOX10 expression in CM but have roles that may be involved with the invasive properties of SOX10-negative cells. Evaluation of multiple independent datasets for different conditions validated our gene signature's ability to determine SOX10 levels and/or activity in both bulk and scRNA-seq data and its usability as a resource for others investigating CM or regulation by SOX10. Our findings suggest that ICi-resistant tumors have more cells lacking SOX10 compared to their treatment-naive counterparts.

Limitations of the study

In this study, we developed a SOX10 gene signature from CM models, so we do not believe that it can differentiate between SOX10-negative malignant and non-malignant cells, such as T cells. This restricted us from incorporating any patient tumor bulk RNA-seq datasets. There were also a limited number of patient samples for some analyses relating to ICi resistance. Only two of the patients in the IHC cohort had matched pre-ICi and ICi-treated samples, and only three patients with pre-ICi samples in the Alvarez-Breckenridge patient scRNA-seq cohort had ICi treatment outcome data.

STAR★METHODS

Detailed methods are provided in the online version of this paper and include the following:

- KEY RESOURCES TABLE
- RESOURCE AVAILABILITY
  - Lead contact
  - Materials availability
  - Data and code availability
- METHOD DETAILS
  - SOX10 signature
  - Bulk RNA-seq
  - Single-cell RNA-seq
  - RNA-seq processing
  - Signature scoring
  - CCLE proteomics data
  - Immunohistochemistry data
- QUANTIFICATION AND STATISTICAL ANALYSIS

SUPPLEMENTAL INFORMATION

Supplemental information can be found online at https://doi.org/10.1016/j.isci.2023.107472.

ACKNOWLEDGMENTS

We thank Dr. Nicole Wilski for valuable feedback during the preparation of this article. We acknowledge the original efforts by Dr. Xiaowei Xu at the University of Pennsylvania for determining H-scores for TMA IHC slides and McKenna Glasheen for curating TMA IHC scores and patient metadata. The Graphical Abstract was created with BioRender.com. This work is supported by grants from the National Institutes of Health (R01 CA196278, R01 CA160495, R01 CA182635) and the Dr. Miriam and Sheldon G. Adelson Medical Research Foundation to A.E. Aplin. The SKCC at Jefferson is supported by the Cancer Center Support Grant, 5P30CA056036, using the Genetics and Translational Pathology Shared Resources. C. Capparelli is supported by American Cancer Society (130042-IRG-16-244-10-IRG), Melanoma Research Foundation, and Legacy of Hope Merit Award.

Financial Support: This work is supported by grants from NIH/NCI (R01 CA196278 and R01 CA160495) to A.E. Aplin. CC is supported by American Cancer Society (130042-IRG-16-244-10-IRG), Melanoma Research Foundation, and Legacy of Hope Merit Award.

AUTHOR CONTRIBUTIONS

T.J.P., C.C., and A.E.A. conceived the study. T.J.P., A.S., and A.E.A. designed the experiments. T.J.P. and A.E.A. analyzed the data. T.J.P. and A.E.A. wrote the manuscript. S.C. edited the manuscript and generated the graphical abstract.

DECLARATION OF INTERESTS

A.E. Aplin has ownership interest in patent number 9880150 and has a pending patent, PCT/US22/76492.

Received: February 16, 2023
Revised: June 18, 2023
Accepted: July 21, 2023
Published: July 25, 2023

REFERENCES

1. Cancer Genome Atlas Network (2015). Genomic Classification of Cutaneous Melanoma. Cell *161*, 1681–1696. https://doi.org/10.1016/j.cell.2015.05.044.

2. Robert, C., Grob, J.J., Stroyakovskiy, D., Karaszewska, B., Hauschild, A., Levchenko, E., Chiarion Sileni, V., Schachter, J., Garbe, C., Bondarenko, I., et al. (2019). Five-Year Outcomes with Dabrafenib plus Trametinib in Metastatic Melanoma. N. Engl. J. Med. *381*, 626–636. https://doi.org/10.1056/NEJMoa1904059.

3. Rambow, F., Rogiers, A., Marin-Bejar, O., Aibar, S., Femel, J., Dewaele, M., Karras, P., Brown, D., Chang, Y.H., Debiec-Rychter, M., et al. (2018). Toward Minimal Residual Disease-Directed Therapy in Melanoma. Cell *174*, 843–855.e19. https://doi.org/10.1016/j.cell.2018.06.025.

4. Shaffer, S.M., Dunagin, M.C., Torborg, S.R., Torre, E.A., Emert, B., Krepler, C., Beqiri, M., Sproesser, K., Brafford, P.A., Xiao, M., et al. (2017). Rare cell variability and drug-induced reprogramming as a mode of cancer drug resistance. Nature *546*, 431–435. https://doi.org/10.1038/nature22794.

5. Sun, C., Wang, L., Huang, S., Heynen, G.J.J.E., Prahallad, A., Robert, C., Haanen, J., Blank, C., Wesseling, J., Willems, S.M., et al. (2014). Reversible and adaptive resistance to BRAF(V600E) inhibition in melanoma. Nature *508*, 118–122. https://doi.org/10.1038/nature13121.

6. Fufa, T.D., Harris, M.L., Watkins-Chow, D.E., Levy, D., Gorkin, D.U., Gildea, D.E., Song, L., Safi, A., Crawford, G.E., Sviderskaya, E.V., et al. (2015). Genomic analysis reveals distinct mechanisms and functional classes of SOX10-regulated genes in melanocytes. Hum. Mol. Genet. *24*, 5433–5450. https://doi.org/10.1093/hmg/ddv267.

7. Mollaaghababa, R., and Pavan, W.J. (2003). The importance of having your SOX on: role of SOX10 in the development of neural crest-derived melanocytes and glia. Oncogene *22*, 3024–3034. https://doi.org/10.1038/sj.onc.1206442.

8. Wegner, M. (2010). All purpose Sox: The many roles of Sox proteins in gene expression. Int. J. Biochem. Cell Biol. *42*, 381–390. https://doi.org/10.1016/j.biocel.2009.07.006.

9. Kanehisa, M., and Goto, S. (2000). KEGG: kyoto encyclopedia of genes and genomes. Nucleic Acids Res. *28*, 27–30. https://doi.org/10.1093/nar/28.1.27.

10. Ashburner, M., Ball, C.A., Blake, J.A., Botstein, D., Butler, H., Cherry, J.M., Davis, A.P., Dolinski, K., Dwight, S.S., Eppig, J.T., et al. (2000). Gene ontology: tool for the unification of biology. The Gene Ontology Consortium. Nat. Genet. *25*, 25–29. https://doi.org/10.1038/75556.

11. Durante, M.A., Kurtenbach, S., Sargi, Z.B., Harbour, J.W., Choi, R., Kurtenbach, S., Goss, G.M., Matsunami, H., and Goldstein, B.J. (2020). Single-cell analysis of olfactory neurogenesis and differentiation in adult humans. Nat. Neurosci. *23*, 323–326. https://doi.org/10.1038/s41593-020-0587-9.

12. Tirosh, I., Izar, B., Prakadan, S.M., Wadsworth, M.H., 2nd, Treacy, D., Trombetta, J.J., Rotem, A., Rodman, C., Lian, C., Murphy, G., et al. (2016). Dissecting the multicellular ecosystem of metastatic melanoma by single-cell RNA-seq. Science *352*, 189–196. https://doi.org/10.1126/science.aad0501.

13. Hugo, W., Zaretsky, J.M., Sun, L., Song, C., Moreno, B.H., Hu-Lieskovan, S., Berent-Maoz, B., Pang, J., Chmielowski, B., Cherry, G., et al. (2016). Genomic and Transcriptomic Features of Response to Anti-PD-1 Therapy in Metastatic Melanoma. Cell *165*, 35–44. https://doi.org/10.1016/j.cell.2016.02.065.

14. Verfaillie, A., Imrichova, H., Atak, Z.K., Dewaele, M., Rambow, F., Hulselmans, G., Christiaens, V., Svetlichnyy, D., Luciani, F., Van den Mooter, L., et al. (2015). Decoding the regulatory landscape of melanoma reveals TEADS as regulators of the invasive cell state. Nat. Commun. *6*, 6683. https://doi.org/10.1038/ncomms7683.

15. Cusanovich, D.A., Pavlovic, B., Pritchard, J.K., and Gilad, Y. (2014). The functional consequences of variation in transcription factor binding. PLoS Genet. *10*, e1004226. https://doi.org/10.1371/journal.pgen.1004226.

16. Pepke, S., Wold, B., and Mortazavi, A. (2009). Computation for ChIP-seq and RNA-seq studies. Nat. Methods *6*, S22–S32. https://doi.org/10.1038/nmeth.1371.

17. Wade, J.T. (2015). Mapping Transcription Regulatory Networks with ChIP-seq and RNA-seq. Adv. Exp. Med. Biol. *883*, 119–134. https://doi.org/10.1007/978-3-319-23603-2_7.

18. Muhammad, I.I., Kong, S.L., Akmar Abdullah, S.N., and Munusamy, U. (2019). RNA-seq and ChIP-seq as Complementary Approaches for Comprehension of Plant Transcriptional Regulatory Mechanism. Int. J. Mol. Sci. *21*, 167. https://doi.org/10.3390/ijms21010167.

19. Morikawa, M., Koinuma, D., Tsutsumi, S., Vasilaki, E., Kanki, Y., Heldin, C.H., Aburatani, H., and Miyazono, K. (2011). ChIP-seq reveals cell type-specific binding patterns of BMP-specific Smads and a novel binding motif. Nucleic Acids Res. *39*, 8712–8727. https://doi.org/10.1093/nar/gkr572.

20. Ghandi, M., Huang, F.W., Jané-Valbuena, J., Kryukov, G.V., Lo, C.C., McDonald, E.R., 3rd, Barretina, J., Gelfand, E.T., Bielski, C.M., Li, H., et al. (2019). Next-generation characterization of the Cancer Cell Line Encyclopedia. Nature *569*, 503–508. https://doi.org/10.1038/s41586-019-1186-3.

21. Larkin, J., Chiarion-Sileni, V., Gonzalez, R., Grob, J.J., Rutkowski, P., Lao, C.D., Cowey, C.L., Schadendorf, D., Wagstaff, J., Dummer, R., et al. (2019). Five-Year Survival with Combined Nivolumab and Ipilimumab in Advanced Melanoma. N. Engl. J. Med. *381*, 1535–1546. https://doi.org/10.1056/NEJMoa1910836.

22. Zaretsky, J.M., Garcia-Diaz, A., Shin, D.S., Escuin-Ordinas, H., Hugo, W., Hu-Lieskovan, S., Torrejon, D.Y., Abril-Rodriguez, G., Sandoval, S., Barthly, L., et al. (2016). Mutations Associated with Acquired Resistance to PD-1 Blockade in Melanoma. N. Engl. J. Med. *375*, 819–829. https://doi.org/10.1056/NEJMoa1604958.

23. Torrejon, D.Y., Abril-Rodriguez, G., Champhekar, A.S., Tsoi, J., Campbell, K.M., Kalbasi, A., Parisi, G., Zaretsky, J.M., Garcia-Diaz, A., Puig-Saus, C., et al. (2020). Overcoming Genetically Based Resistance Mechanisms to PD-1 Blockade. Cancer Discov. *10*, 1140–1157. https://doi.org/10.1158/2159-8290.CD-19-1409.

24. Sade-Feldman, M., Yizhak, K., Bjorgaard, S.L., Ray, J.P., de Boer, C.G., Jenkins, R.W., Lieb, D.J., Chen, J.H., Frederick, D.T., Barzily-Rokni, M., et al. (2018). Defining T Cell States Associated with Response to Checkpoint Immunotherapy in Melanoma. Cell *175*, 998–1013.e20. https://doi.org/10.1016/j.cell.2018.10.038.

25. Li, H., van der Leun, A.M., Yofe, I., Lubling, Y., Gelbard-Solodkin, D., van Akkooi, A.C.J., van den Braber, M., Rozeman, E.A., Haanen, J.B.A.G., Blank, C.U., et al. (2020). Dysfunctional CD8 T Cells Form a Proliferative, Dynamically Regulated Compartment within Human Melanoma. Cell *181*, 747. https://doi.org/10.1016/j.cell.2020.04.017.

26. Smalley, I., Chen, Z., Phadke, M., Li, J., Yu, X., Wyatt, C., Evernden, B., Messina, J.L., Sarnaik, A., Sondak, V.K., et al. (2021).

Single-Cell Characterization of the Immune Microenvironment of Melanoma Brain and Leptomeningeal Metastases. Clin. Cancer Res. *27*, 4109–4125. https://doi.org/10.1158/1078-0432.CCR-21-1694.

27. Haas, L., Elewaut, A., Gerard, C.L., Umkehrer, C., Leiendecker, L., Pedersen, M., Krecioch, I., Hoffmann, D., Novatchkova, M., Kuttke, M., et al. (2021). Acquired resistance to anti-MAPK targeted therapy confers an immune-evasive tumor microenvironment and cross-resistance to immunotherapy in melanoma. Nat. Cancer *2*, 693–708. https://doi.org/10.1038/s43018-021-00221-9.

28. Horn, L.A., Fousek, K., and Palena, C. (2020). Tumor Plasticity and Resistance to Immunotherapy. Trends Cancer *6*, 432–441. https://doi.org/10.1016/j.trecan.2020.02.001.

29. Capparelli, C., Purwin, T.J., Glasheen, M., Caksa, S., Tiago, M., Wilski, N., Pomante, D., Rosenbaum, S., Nguyen, M.Q., Cai, W., et al. (2022). Targeting SOX10-deficient cells to reduce the dormant-invasive phenotype state in melanoma. Nat. Commun. *13*, 1381. https://doi.org/10.1038/s41467-022-28801-y.

30. Eskiocak, B., McMillan, E.A., Mendiratta, S., Kollipara, R.K., Zhang, H., Humphries, C.G., Wang, C., Garcia-Rodriguez, J., Ding, M., Zaman, A., et al. (2017). Biomarker Accessible and Chemically Addressable Mechanistic Subtypes of BRAF Melanoma. Cancer Discov. *7*, 832–851. https://doi.org/10.1158/2159-8290.CD-16-0955.

31. Wouters, J., Kalender-Atak, Z., Minnoye, L., Spanier, K.I., De Waegeneer, M., Bravo González-Blas, C., Mauduit, D., Davie, K., Hulselmans, G., Najem, A., et al. (2020). Robust gene expression programs underlie recurrent cell states and phenotype switching in melanoma. Nat. Cell Biol. *22*, 986–998. https://doi.org/10.1038/s41556-020-0547-3.

32. Aibar, S., González-Blas, C.B., Moerman, T., Huynh-Thu, V.A., Imrichova, H., Hulselmans, G., Rambow, F., Marine, J.C., Geurts, P., Aerts, J., et al. (2017). SCENIC: single-cell regulatory network inference and clustering. Nat. Methods *14*, 1083–1086. https://doi.org/10.1038/nmeth.4463.

33. Subramanian, A., Tamayo, P., Mootha, V.K., Mukherjee, S., Ebert, B.L., Gillette, M.A., Paulovich, A., Pomeroy, S.L., Golub, T.R., Lander, E.S., and Mesirov, J.P. (2005). Gene set enrichment analysis: a knowledge-based approach for interpreting genome-wide expression profiles. Proc Natl Acad Sci USA *102*, 15545–15550. https://doi.org/10.1073/pnas.0506580102.

34. Sherman, B.T., Hao, M., Qiu, J., Jiao, X., Baseler, M.W., Lane, H.C., Imamichi, T., and Chang, W. (2022). DAVID: a web server for functional enrichment analysis and functional annotation of gene lists (2021 update). Nucleic Acids Res. *50*, W216–W221. https://doi.org/10.1093/nar/gkac194.

35. Mootha, V.K., Lindgren, C.M., Eriksson, K.F., Subramanian, A., Sihag, S., Lehar, J., Puigserver, P., Carlsson, E., Ridderstråle, M., Laurila, E., et al. (2003). PGC-1alpha-responsive genes involved in oxidative phosphorylation are coordinately downregulated in human diabetes. Nat. Genet. *34*, 267–273. https://doi.org/10.1038/ng1180.

36. Kharchenko, P.V., Silberstein, L., and Scadden, D.T. (2014). Bayesian approach to single-cell differential expression analysis. Nat. Methods *11*, 740–742. https://doi.org/10.1038/nmeth.2967.

37. Tsoi, J., Robert, L., Paraiso, K., Galvan, C., Sheu, K.M., Lay, J., Wong, D.J.L., Atefi, M., Shirazi, R., Wang, X., et al. (2018). Multi-stage Differentiation Defines Melanoma Subtypes with Differential Vulnerability to Drug-Induced Iron-Dependent Oxidative Stress. Cancer Cell *33*, 890–904.e5. https://doi.org/10.1016/j.ccell.2018.03.017.

38. Barbie, D.A., Tamayo, P., Boehm, J.S., Kim, S.Y., Moody, S.E., Dunn, I.F., Schinzel, A.C., Sandy, P., Meylan, E., Scholl, C., et al. (2009). Systematic RNA interference reveals that oncogenic KRAS-driven cancers require TBK1. Nature *462*, 108–112. https://doi.org/10.1038/nature08460.

39. Nusinow, D.P., Szpyt, J., Ghandi, M., Rose, C.M., McDonald, E.R., 3rd, Kalocsay, M., Jané-Valbuena, J., Gelfand, E., Schweppe, D.K., Jedrychowski, M., et al. (2020). Quantitative Proteomics of the Cancer Cell Line Encyclopedia. Cell *180*, 387–402.e16. https://doi.org/10.1016/j.cell.2019.12.023.

40. Hartsough, E.J., Kugel, C.H.,, 3rd, Aplin, A.E., Vido, M.J., Berger, A.C., Purwin, T.J., Goldberg, A., Davies, M.A., Schiewer, M.J., Knudsen, K.E., et al. (2018). Response and Resistance to Paradox-Breaking BRAF Inhibitor in Melanomas In Vivo and Ex Vivo. Mol. Cancer Ther. *17*, 84–95. https://doi.org/10.1158/1535-7163.MCT-17-0705.

41. Sanchez, I.M., Purwin, T.J., Chervoneva, I., Erkes, D.A., Nguyen, M.Q., Davies, M.A., Nathanson, K.L., Kemper, K., Peeper, D.S., and Aplin, A.E. (2019). In Vivo ERK1/2 Reporter Predictively Models Response and Resistance to Combined BRAF and MEK Inhibitors in Melanoma. Mol. Cancer Ther. *18*, 1637–1648. https://doi.org/10.1158/1535-7163.MCT-18-1056.

42. Schmidt, M., Mortensen, L.S., Loeffler-Wirth, H., Kosnopfel, C., Krohn, K., Binder, H., and Kunz, M. (2021). Single-cell trajectories of melanoma cell resistance to targeted treatment. Cancer Biol. Med. *19*, 56–73. https://doi.org/10.20892/j.issn.2095-3941.2021.0267.

43. Alvarez-Breckenridge, C., Markson, S.C., Stocking, J.H., Nayyar, N., Lastrapes, M., Strickland, M.R., Kim, A.E., de Sauvage, M., Dahal, A., Larson, J.M., et al. (2022). Microenvironmental Landscape of Human Melanoma Brain Metastases in Response to Immune Checkpoint Inhibition. Cancer Immunol. Res. *10*, 996–1012. https://doi.org/10.1158/2326-6066.CIR-21-0870.

44. Jerby-Arnon, L., Shah, P., Cuoco, M.S., Rodman, C., Su, M.J., Melms, J.C., Leeson, R., Kanodia, A., Mei, S., Lin, J.R., et al. (2018). A Cancer Cell Program Promotes T Cell Exclusion and Resistance to Checkpoint Blockade. Cell *175*, 984–997.e24. https://doi.org/10.1016/j.cell.2018.09.006.

45. Zerbino, D.R., Wilder, S.P., Johnson, N., Juettemann, T., and Flicek, P.R. (2015). The ensembl regulatory build. Genome Biol. *16*, 56. https://doi.org/10.1186/s13059-015-0621-5.

46. Mogha, A., Benesh, A.E., Patra, C., Engel, F.B., Schöneberg, T., Liebscher, I., and Monk, K.R. (2013). Gpr126 functions in Schwann cells to control differentiation and myelination via G-protein activation. J. Neurosci. *33*, 17976–17985. https://doi.org/10.1523/JNEUROSCI.1809-13.2013.

47. Finzsch, M., Schreiner, S., Kichko, T., Reeh, P., Tamm, E.R., Bösl, M.R., Meijer, D., and Wegner, M. (2010). Sox10 is required for Schwann cell identity and progression beyond the immature Schwann cell stage. J. Cell Biol. *189*, 701–712. https://doi.org/10.1083/jcb.200912142.

48. Prasad, M.K., Reed, X., Gorkin, D.U., Cronin, J.C., McAdow, A.R., Chain, K., Hodonsky, C.J., Jones, E.A., Svaren, J., Antonellis, A., et al. (2011). SOX10 directly modulates ERBB3 transcription via an intronic neural crest enhancer. BMC Dev. Biol. *11*, 40. https://doi.org/10.1186/1471-213X-11-40.

49. Bravo González-Blas, C., Minnoye, L., Papasokrati, D., Aibar, S., Hulselmans, G., Christiaens, V., Davie, K., Wouters, J., and Aerts, S. (2019). cisTopic: cis-regulatory topic modeling on single-cell ATAC-seq data. Nat. Methods *16*, 397–400. https://doi.org/10.1038/s41592-019-0367-1.

50. Rok, J., Rzepka, Z., Kowalska, J., Banach, K., Beberok, A., and Wrześniok, D. (2022). The Anticancer Potential of Doxycycline and Minocycline-A Comparative Study on Amelanotic Melanoma Cell Lines. Int. J. Mol. Sci. *23*, 831. https://doi.org/10.3390/ijms23020831.

51. Arikawa, K., Takuwa, N., Yamaguchi, H., Sugimoto, N., Kitayama, J., Nagawa, H., Takehara, K., and Takuwa, Y. (2003). Ligand-dependent inhibition of B16 melanoma cell migration and invasion via endogenous S1P2 G protein-coupled receptor. Requirement of inhibition of cellular RAC activity. J. Biol. Chem. *278*, 32841–32851. https://doi.org/10.1074/jbc.M305024200.

52. Paavola, K.J., Sidik, H., Zuchero, J.B., Eckart, M., and Talbot, W.S. (2014). Type IV collagen is an activating ligand for the adhesion G protein-coupled receptor GPR126. Sci. Signal. *7*, ra76. https://doi.org/10.1126/scisignal.2005347.

53. Rosenbaum, S.R., Tiago, M., Caksa, S., Capparelli, C., Purwin, T.J., Kumar, G., Glasheen, M., Pomante, D., Kotas, D., Chervoneva, I., and Aplin, A.E. (2021). SOX10 requirement for melanoma tumor growth is due, in part, to immune-mediated effects. Cell Rep. *37*, 110085. https://doi.org/10.1016/j.celrep.2021.110085.

54. Abou-Hamad, J., Hodgins, J.J., de Souza, C.T., Garland, B., Labrèche, C., Marotel, M., Gibson, C., Delisle, S., Pascoal, J., Auer, R.C., et al. (2022). CEACAM1 is a direct SOX10 target and inhibits melanoma immune infiltration and stemness. iScience *25*, 105524. https://doi.org/10.1016/j.isci.2022.105524.

55. Yokoyama, S., Takahashi, A., Kikuchi, R., Nishibu, S., Lo, J.A., Hejna, M., Moon, W.M., Kato, S., Zhou, Y., Hodi, F.S., et al. (2021). SOX10 Regulates Melanoma Immunogenicity through an IRF4-IRF1 Axis. Cancer Res. *81*, 6131–6141. https://doi.org/10.1158/0008-5472.CAN-21-2078.

56. Karras, P., Bordeu, I., Pozniak, J., Nowosad, A., Pazzi, C., Van Raemdonck, N., Landeloos, E., Van Herck, Y., Pedri, D., Bervoets, G., et al. (2022). A cellular hierarchy in melanoma uncouples growth and metastasis. Nature *610*, 190–198. https://doi.org/10.1038/s41586-022-05242-7.

57. Kalaora, S., Wolf, Y., Feferman, T., Barnea, E., Greenstein, E., Reshef, D., Tirosh, I., Reuben, A., Patkar, S., Levy, R., et al. (2018). Combined Analysis of Antigen Presentation and T-cell Recognition Reveals Restricted Immune Responses in Melanoma. Cancer Discov. *8*, 1366–1375. https://doi.org/10.1158/2159-8290.CD-17-1418.

58. Frangieh, C.J., Melms, J.C., Thakore, P.I., Geiger-Schuller, K.R., Ho, P., Luoma, A.M., Cleary, B., Jerby-Arnon, L., Malu, S., Cuoco, M.S., et al. (2021). Multimodal pooled Perturb-CITE-seq screens in patient models define mechanisms of cancer immune evasion. Nat. Genet. *53*, 332–341. https://doi.org/10.1038/s41588-021-00779-1.

59. Landsberg, J., Kohlmeyer, J., Renn, M., Bald, T., Rogava, M., Cron, M., Fatho, M., Lennerz, V., Wölfel, T., Hölzel, M., and Tüting, T. (2012). Melanomas resist T-cell therapy through inflammation-induced reversible dedifferentiation. Nature *490*, 412–416. https://doi.org/10.1038/nature11538.

60. Patel, S.J., Sanjana, N.E., Kishton, R.J., Eidizadeh, A., Vodnala, S.K., Cam, M., Gartner, J.J., Jia, L., Steinberg, S.M., Yamamoto, T.N., et al. (2017). Identification of essential genes for cancer immunotherapy. Nature *548*, 537–542. https://doi.org/10.1038/nature23477.

61. Yamshchikov, G.V., Mullins, D.W., Chang, C.C., Ogino, T., Thompson, L., Presley, J., Galavotti, H., Aquila, W., Deacon, D., Ross, W., et al. (2005). Sequential immune escape and shifting of T cell responses in a long-term survivor of melanoma. J. Immunol. *174*, 6863–6871. https://doi.org/10.4049/jimmunol.174.11.6863.

62. Sharon, C.E., and Karakousis, G.C. (2022). Educational Review: Neoadjuvant Approaches to Melanoma. Ann. Surg Oncol. *29*, 8492–8500. https://doi.org/10.1245/s10434-022-12224-6.

63. Ishihara, J., Fukunaga, K., Ishihara, A., Larsson, H.M., Potin, L., Hosseinchi, P., Galliverti, G., Swartz, M.A., and Hubbell, J.A. (2017). Matrix-binding checkpoint immunotherapies enhance antitumor efficacy and reduce adverse events. Sci. Transl. Med. *9*, eaan0401. https://doi.org/10.1126/scitranslmed.aan0401.

64. Zhong, W., Myers, J.S., Wang, F., Wang, K., Lucas, J., Rosfjord, E., Lucas, J., Hooper, A.T., Yang, S., Lemon, L.A., et al. (2020). Comparison of the molecular and cellular phenotypes of common mouse syngeneic models with human tumors. BMC Genom. *21*, 2. https://doi.org/10.1186/s12864-019-6344-3.

65. Frankish, A., Diekhans, M., Ferreira, A.M., Johnson, R., Jungreis, I., Loveland, J., Mudge, J.M., Sisu, C., Wright, J., Armstrong, J., et al. (2019). GENCODE reference annotation for the human and mouse genomes. Nucleic Acids Res. *47*, D766–D773. https://doi.org/10.1093/nar/gky955.

66. Yevshin, I., Sharipov, R., Kolmykov, S., Kondrakhin, Y., and Kolpakov, F. (2019). GTRD: a database on gene transcription regulation-2019 update. Nucleic Acids Res. *47*, D100–D105. https://doi.org/10.1093/nar/gky1128.

67. Dobin, A., Davis, C.A., Schlesinger, F., Drenkow, J., Zaleski, C., Jha, S., Batut, P., Chaisson, M., and Gingeras, T.R. (2013). STAR: ultrafast universal RNA-seq aligner. Bioinformatics *29*, 15–21. https://doi.org/10.1093/bioinformatics/bts635.

68. Li, B., and Dewey, C.N. (2011). RSEM: accurate transcript quantification from RNA-Seq data with or without a reference genome. BMC Bioinf. *12*, 323. https://doi.org/10.1186/1471-2105-12-323.

69. Putri, G.H., Anders, S., Pyl, P.T., Pimanda, J.E., and Zanini, F. (2022). Analysing high-throughput sequencing data in Python with HTSeq 2.0. Bioinformatics *38*, 2943–2945. https://doi.org/10.1093/bioinformatics/btac166.

70. Zheng, G.X.Y., Terry, J.M., Belgrader, P., Ryvkin, P., Bent, Z.W., Wilson, R., Ziraldo, S.B., Wheeler, T.D., McDermott, G.P., Zhu, J., et al. (2017). Massively parallel digital transcriptional profiling of single cells. Nat. Commun. *8*, 14049. https://doi.org/10.1038/ncomms14049.

71. Leinonen, R., Sugawara, H., and Shumway, M.; International Nucleotide Sequence Database Collaboration (2011). The sequence read archive. Nucleic Acids Res. *39*, D19–D21. https://doi.org/10.1093/nar/gkq1019.

72. Katz, K., Shutov, O., Lapoint, R., Kimelman, M., Brister, J.R., and O'Sullivan, C. (2022). The Sequence Read Archive: a decade more of explosive growth. Nucleic Acids Res. *50*, D387–D390. https://doi.org/10.1093/nar/gkab1053.

73. Lawrence, M., Gentleman, R., and Carey, V. (2009). rtracklayer: an R package for interfacing with genome browsers. Bioinformatics *25*, 1841–1842. https://doi.org/10.1093/bioinformatics/btp328.

74. Stuart, T., Butler, A., Hoffman, P., Hafemeister, C., Papalexi, E., Mauck, W.M., 3rd, Hao, Y., Stoeckius, M., Smibert, P., and Satija, R. (2019). Comprehensive Integration of Single-Cell Data. Cell *177*, 1888–1902.e21. https://doi.org/10.1016/j.cell.2019.05.031.

75. Hänzelmann, S., Castelo, R., and Guinney, J. (2013). GSVA: gene set variation analysis for microarray and RNA-seq data. BMC Bioinf. *14*, 7. https://doi.org/10.1186/1471-2105-14-7.

76. Love, M.I., Huber, W., and Anders, S. (2014). Moderated estimation of fold change and dispersion for RNA-seq data with DESeq2. Genome Biol. *15*, 550. https://doi.org/10.1186/s13059-014-0550-8.

77. Robinson, M.D., McCarthy, D.J., and Smyth, G.K. (2010). edgeR: a Bioconductor package for differential expression analysis of digital gene expression data. Bioinformatics *26*, 139–140. https://doi.org/10.1093/bioinformatics/btp616.

78. Lötsch, J., Malkusch, S., and Ultsch, A. (2021). Optimal distribution-preserving downsampling of large biomedical data sets (opdisDownsampling). PLoS One *16*, e0255838. https://doi.org/10.1371/journal.pone.0255838.

79. Kolde, R. (2012). Pheatmap: pretty heatmaps. R package version *1*, 726.

80. Krepler, C., Sproesser, K., Brafford, P., Beqiri, M., Garman, B., Xiao, M., Shannan, B., Watters, A., Perego, M., Zhang, G., et al. (2017). A Comprehensive Patient-Derived Xenograft Collection Representing the Heterogeneity of Melanoma. Cell Rep. *21*, 1953–1967. https://doi.org/10.1016/j.celrep.2017.10.021.

STAR★METHODS

KEY RESOURCES TABLE

REAGENT or RESOURCE	SOURCE	IDENTIFIER
Deposited data		
Human reference genome NCBI build 38, GRCh38	Genome Reference Consortium	http://www.ncbi.nlm.nih.gov/projects/genome/assembly/grc/human/
GENCODE	The Human GENCODE Gene Set[65]	https://www.gencodegenes.org/human/releases.html
GRCh38-2020-A reference transcriptome	10X Genomics	https://support.10xgenomics.com/single-cell-gene-expression/software/downloads/latest
Ensembl Regulatory Build (v101)	Zerbino et al.[45]	https://ftp.ensembl.org/pub/release-101/regulation/
CCLE Proteomics	Nusinow et al.[39]	https://www.cell.com/cms/10.1016/j.cell.2019.12.023/attachment/3709dedc-3a01-4e1d-ab4c-82597295c5d2/mmc2.xlsx
SOX10 ChIP-seq (v20.06)	Gene Transcription Regulation Database Yevshin et al.[66]	https://gtrd.biouml.org/#! Experiment: EXP034107
Raw counts for SOX10KD ATAC-seq	González-Blas et al.[49]	GEO: GSE114557
Raw reads for MeWo gSOX10 bulk RNA-seq	Capparelli et al.[29]	SRA: SRP306463
Raw reads for A375 gSOX10 bulk RNA-seq	Capparelli et al.[29]	SRA: SRP329298
Raw counts for Wouters SOX10 KD bulk RNA-seq	Wouters et al.[31]	GEO: GSE134432
Raw reads for Sun SOX10 KD bulk RNA-seq	Sun et al.[5]	SRA: SRP029434
RSEM counts for DepMap RNA-seq (v20Q1)	Ghandi et al.[20]	https://doi.org/10.6084/m9.figshare.11791698.v3
Raw reads for Tsoi cell line panel bulk RNA-seq	Tsoi et al.[37]	SRA: SRP074198
Raw reads for PBRT BRAFi-resistant bulk RNA-seq	Capparelli et al.[29]	SRA: SRP329297
Raw reads for CRT BRAFi+MEKi-resistant bulk RNA-seq	Capparelli et al.[29]	SRA: SRP329298
Loom files with raw counts for Wouters scRNA-seq SOX10 KD dataset	Wouters et al.[31]	http://scope.aertslab.org/#/Wouters_Human_Melanoma
Loom file with raw counts for Wouters scRNA-seq cell line panel dataset	Wouters et al.[31]	http://scope.aertslab.org/#/Wouters_Human_Melanoma
Raw reads for A375 parental and BRAFi −/+ MEKi-resistant scRNA-seq samples	Schmidt and Mortensen et al.[42]	SRA: SRP301922
Cell type calls and raw counts data for Alvarez-Breckenridge scRNA-seq patient	Alvarez-Breckenridge et al.[43]	https://portals.broadinstitute.org/single_cell/study/microenvironmental-correlates-of-immune-checkpoint-inhibitor-response-in-human-melanoma-brain-metastases-revealed-by-t-cell-receptor-and-single-cell-rna-sequencing
Cell type calls data for Jerby-Arnon scRNA-seq patient dataset	Jerby-Arnon et al.[44]	https://portals.broadinstitute.org/single_cell/study/melanoma-immunotherapy-resistance
Raw counts data for Jerby-Arnon scRNA-seq patient dataset	Jerby-Arnon et al.[44]	GEO: GSE115978
Wouters Gene Signatures	Wouters et al.[31]	Network Data Exchange NDEx (https://doi.org/10.18119/N91W2T)

(*Continued on next page*)

Continued

REAGENT or RESOURCE	SOURCE	IDENTIFIER
mSigDB Gene Signature (v7.2)	Subramanian et al.[33]	http://www.gsea-msigdb.org/gsea/msigdb/cards/SOX10_TARGET_GENES
Eskiocak Gene Signature	Eskiocak et al.[30]	https://aacr.silverchair-cdn.com/aacr/content_public/journal/cancerdiscovery/7/8/10.1158_2159-8290.cd-16-0955/5/21598290cd160955-sup-171064_4_unknown_upload_3998923_88x029.xlsx
SOX10 IHC staining data	Capparelli et al.[29]	N/A
Software and algorithms		
Star	Dobin et al.[67]	https://github.com/alexdobin/STAR
RSEM	Li et al.[68]	https://github.com/deweylab/RSEM
HTSeq	Putri et al.[69]	https://htseq.readthedocs.io/en/master/
CellRanger	10X Genomics Zheng et al.[70]	https://support.10xgenomics.com/single-cell-gene-expression/software
SCopeLoomR v0.10.2	Aibar et al.[32]	https://github.com/aertslab/SCopeLoomR
SRA toolkit v2.10.4	Leinonen et al.[71] Katz et al.[72]	https://github.com/ncbi/sra-tools
R	The R Project for Statistical Computing	https://www.R-project.org
rtracklayer	Lawrence et al.[73]	https://bioconductor.org/packages/rtracklayer/
liftOver	Bioconductor	https://bioconductor.org/packages/liftOver
Seurat	Stuart and Butler et al.[74]	https://satijalab.org/seurat/
GSEABase	Bioconductor	https://bioconductor.org/packages/GSEABase
GSVA	Hanzelmann et al.[75]	https://bioconductor.org/packages/GSVA
AUCell	Aibar et al.[32]	https://bioconductor.org/packages/AUCell
DESeq2	Love et al.[76]	https://bioconductor.org/packages/DESeq2/
EdgeR	Robinson et al.[77]	https://bioconductor.org/packages/edgeR
stats package	The R Project for Statistical Computing	https://www.R-project.org
opdisDownsampling (v0.8.2)	Lotsch et al.[78]	https://cran.r-project.org/package=opdisDownsampling
multimode	N/A	https://cran.r-project.org/package=multimode
VennDiagram	N/A	https://CRAN.R-project.org/package=VennDiagram
ggplot2	N/A	https://CRAN.R-project.org/package=ggplot2
pheatmap	Kolde et al.[79]	https://CRAN.R-project.org/package=pheatmap
GSEA	Mootha et al.[35] Subramanian et al.[33]	https://www.gsea-msigdb.org/gsea/index.jsp
Database for Annotation, Visualization and Integrated Discovery (DAVID)	Sherman et al.[34]	https://david.ncifcrf.gov

RESOURCE AVAILABILITY

Lead contact

Further information and requests for resources and reagents should be directed to and will be fulfilled by the Lead Contact, Andrew E. Aplin (Andrew.Aplin@Jefferson.edu).

Materials availability

This study did not generate new unique reagents.

Data and code availability

- This paper analyzes existing, publicly available data. These accession numbers for the datasets are listed in the key resources table. All data reported in this paper will be shared by the lead contact upon request.
- This paper does not report original code.
- Any additional information required to reanalyze the data reported in this paper is available from the lead contact upon request.

METHOD DETAILS

SOX10 signature

Gene and regulatory data

Gene regulation (Ensembl v101)[45] and transcript (GENCODE v30)[65] annotation data were obtained for the human reference genome build GRCh38. Transcript-promoter matches were defined by transcription start sites occurring within the promoter boundary regions of an ensemble promoter regulatory ID. From 613,944 regulatory entries, 35,191 promoter regions matched with 121,111 transcripts from 27,090 genes.

ChIP-seq

SOX10 ChIP-seq data were obtained from the Gene Transcription Regulation Database (GTRD).[66] From a total of 7,396 ChIP-seq peaks, 362 peaks overlapped 353 promoter regions. The 353 promoter regions matched with 1,977 unique transcripts from 501 genes.

SOX10 knockdown ATAC-seq

ATAC-seq merged peaks raw counts data for SOX10 time-series knockdown and control samples from two melanoma cell lines[49] were obtained from the Gene Expression Omnibus (GEO) under the accession number GSE114557. DESeq2[76] was used to generate normalized abundance counts. SOX10 ChIP-seq GRCh38 reference build data were converted to GRCh19 coordinates using the rtracklayer[73] and liftOver packages. 346 peaks (477 genes) of the 362 ChIP-seq peaks overlapped 341 ATAC-seq peaks with abundance data. 332 peaks (461 genes) were consistently down-regulated at 24, 48 and 72 h following SOX10 knockdown when compared to control.

gSOX10 RNA-seq

Raw RNA-seq reads for 18 samples from parental and SOX10-null CRISPR guide RNAs (gSOX10 #2 and #4) for A375 and MeWo cell lines were obtained from the Sequence Read Archive (SRA) under the accession numbers SRP306463 and SRP329298 using the SRA toolkit (v 2.10.4).[71,72] Data were processed from raw sequencing data as described below in the RNA-seq Processing section. Pairwise comparisons were performed for each gSOX10 vs. parental cell line.

Refined SOX10 signatures

A prioritized list of genes was limited to the 501 genes identified as having a SOX10 ChIP-seq peak overlapping the promoter. A SOX10 gene signature list was generated based on all four gSOX10 vs. parental comparisons consistently showing significant (BHFDR <0.05) down-regulation. These sets were further refined to those consistently down-regulated in the ATAC-seq data. The 30 genes significantly down-regulated in all cell line comparisons also had lower ATAC-seq abundance after SOX10 knockdown. Venn diagrams were generated using the VennDiagram package (v1.6.20 https://CRAN.R-project.org/package=VennDiagram). DAVID[34] was used to determine enriched Gene Ontology biological processes gene sets.[10]

Bulk RNA-seq

CCLE RNA-seq

RNA-seq RSEM counts data were downloaded from DepMap (v 20Q1 https://depmap.org/portal/download). Data were reduced to 62 cutaneous melanoma cell lines prior to further processing. Heatmaps were generated using the pheatmap package (v1.0.12).[79]

SOX10 knockdown, cell line panel and targeted therapy-resistant RNA-seq

Raw counts data for six cell lines with SOX10 knockdown and control samples were obtained from the GEO under the accession number GSE134432. A paired-sample comparison model was used to calculate differentially expressed genes. Raw RNA-seq reads for three parental & SOX10 knockdown samples, a panel of 53 CM cell lines, six parental & BRAFi-resistant samples, and nine parental & BRAFi + MEKi-resistant samples were gathered from the SRA for accession numbers SRP029434, SRP074198, SRP329297, and SRP329298, respectively, using the SRA toolkit (v 2.10.4).[71,72]

Single-cell RNA-seq

SOX10 knockdown and cell line panel datasets

Loom files containing gene expression data for ten cell lines and SOX10 knockdown datasets originating from Wouters et al.[31] were obtained from SCope (http://scope.aertslab.org/#/Wouters_Human_Melanoma). SCopeLoomR[32] (v0.10.2 https://github.com/aertslab/SCopeLoomR) was used to load data into R.

MAPKi-resistant dataset

Raw RNA Sequencing reads for four treatment-naïve or BRAFi -/+ MEKi A375 cell line samples originating from Schmidt and Mortensen et al.[42] were obtained from the SRA under the accession number SRP301922 using the SRA toolkit (v 2.10.4).[71,72]

Jerby-Arnon ICi-Resistant dataset

Raw gene expression counts and cell type data for malignant cells from unmatched treatment-naïve (n=7) and ICi-resistant (n=7) melanoma patient tumors originating from Jerby-Arnon et al.[44] were gathered from GEO under the accession number GSE115978 and the Single-Cell Portal (https://portals.broadinstitute.org/single_cell/study/melanoma-immunotherapy-resistance), respectively.

Alvarez-Breckenridge ICi-Resistant dataset

Raw counts gene expression and cell type data for malignant cells from metastatic brain melanoma tumors originating from Alvarez-Breckenridge et al.[43] were gathered from the Single-Cell Portal. Tumor samples with at least 50 malignant cells were used for further analyses. Of the three ICi-naïve patients that later received ICi (Pre-ICi), one was a Responder and the others were Non-responders.[43] Two of the ICi-naïve patients received radiotherapy prior to resection. Post-ICi samples were grouped by visually interpreting the patients' systemic therapy at the time of resection,[43] resulting in ICi-naïve (n=8), On MAPKi (n=2), On ICi (n=6) and Off ICi (n=12) tumor samples.

RNA-seq processing

Bulk RNA-seq

Raw RNA Sequencing reads were aligned to the GRCh38 human reference genome using Star[67] and GENCODE[65] annotations. RSEM[68] or HTSeq[69] was used to quantify gene level expression for paired-end and single-end sequencing samples, respectively. Gene normalization and differential expression analyses were performed using DESeq2.[76]

Single-cell RNA-seq

CellRanger[70] was used to quantify gene expression levels, aggregate data and filter empty cell barcodes for raw RNA sequencing reads from 10x Genomics samples for the MAPKi-resistant scRNA-seq dataset. The 10x GRCh38-2020-A reference genome was used for mapping reads. Cells with at least 1,000 features and less than 10 percent expression of mitochondrial genes were retained for further analyses for the MAPKi-resistant scRNA-seq dataset. Malignant cells from tumors with at least 50 malignant cells were retained for both the Jerby-Arnon and Alvarez-Breckenridge datasets. Raw counts data were normalized via Seurat[74] using the NormalizeData function with the default "LogNormalize" method and 10,000 scale factor settings for the MAPKi-resistant, Jerby-Arnon and Alvarez-Breckenridge scRNA-seq datasets. Log2-transformed pseudo counts per million data were generated using the edgeR package[77] for the Cell Line Panel scRNA-seq data. Down-sampling of patient tumor scRNA-seq data were performed using the opdisDownsampling package (v 0.8.2) (https://cran.r-project.org/package=opdisDownsampling).[78]

Signature scoring

GSEA

GSEA[33,35] was used to identify enrichment of gene sets. As default, the "Signal2Noise" weighted enrichment statistic was performed after removing non-expressed genes, producing normalized counts and collapsing from Ensembl to human gene identifiers. When described, the GSEA pre-ranked method was performed using either log2-transformed ratio values or DESeq2 Wald's test statistic values after filtering out zero or "NA" values. A total of 1,000 permutations were performed using gene sets, and p-values equaling zero are reported as less than 0.001.

ssGSEA

The single-sample GSEA (ssGSEA)[38] method was used to calculate gene set scores for bulk RNA-seq using the gsva (v1.40.1)[75] package. The multimode package (https://cran.r-project.org/package=multimode) was used to test for uni-modality and identify the anti-modal position for bimodal data.

AUCell

Gene set scores for scRNA-seq data were calculated using the AUCell (v1.14.0)[32] package. Thresholds were adjusted to correlate SOX10-expressing cells with SOX10 activity scores. The ggplot2 package (https://CRAN.R-project.org/package=ggplot2) was used to generate violin plots.

CCLE proteomics data

SOX10 (P56693) relative protein expression data were downloaded from DepMap (https://depmap.org/portal). The proteomics data originated from Nusinow et al.[39]

Immunohistochemistry data

SOX10 IHC staining data were collected from Capparelli et al.[29] The percentage of cancer cells expressing none, low, medium, or high levels of SOX10 was previously quantified by a trained pathologist.[29] Patient clinical data were retrieved from Krepler et al.[80] IHC samples from patients without any past treatment listed were considered treatment-naïve (n=22). A total of 20 samples were from patients that received ICi therapy. Three were excluded due to patients either stopping ICi therapy because of adverse events (n=1) or not having clinical response and treatment status information (n=2). Samples from patients on ICi but without clinical response information were grouped as "Ongoing" (n=3). Samples were grouped into complete responders (CR) (n=2) and progressive or stable disease (PD/SD) (n=12) using the latest clinical response information available for ICi therapies. Two of the PD samples were collected after 1-2 cycles of ICi therapy, while one patient with SD remained on ICi treatment. Three patients had samples from different timepoints.

QUANTIFICATION AND STATISTICAL ANALYSIS

The Pearson's product-moment correlation coefficient, Spearman's rho and Wilcoxon rank sum test with continuity correction (aka 'Mann-Whitney' test) were performed using the stats package (v 4.1.2) in R (v 4.1.2 https://www.R-project.org). A *p-value* < 0.05 was considered statistically significant (*$p<0.05$, **$p<0.01$, ***$p<0.001$, NS Not Significant), as described in the figure legends. Violin plots contain box and whiskers (interquartile range, median and minimum/maximum values).